

# Modified model for harmonic generation free electron laser

DENG Haixiao<sup>\*</sup> DAI Zhimin

*Shanghai Institute of Applied Physics, Shanghai 201800, China*

**Abstract** The longitudinal modulation to the electron beam by a coherent seed laser pulse is widely used for generating fully coherent, short wavelength radiation in various harmonic generation free electron laser (FEL) schemes. After introducing the density modulation, microstructures down to attosecond scale are produced over the distance of one seed laser wavelength. In order to take into account the microstructures in the theoretical and numerical analysis, in the frame of undulator period averaged approach, a modified model for harmonic generation FEL is developed in this paper. With the modified model, three harmonic generation FEL examples are investigated by employing Shanghai soft X-ray FEL (SXFEL) parameters. In FEL schemes with ultra-high harmonic generation and ultra-short pulse, the modified model presents some interesting aspects which are helpful for understanding of radiation pulse evolution, bunching efficiency and noise propagation issues.

**Key words** FEL, Harmonic, Model, Attosecond

## 1 Introduction

Today, various free electron laser (FEL) schemes<sup>[1–5]</sup> based on harmonic generation of the external seed laser are competitive and affordable to compact and fully coherent radiation sources in the short-wavelength region. In harmonic generation FEL, the external seed laser and the electron beam interacts with each other in the first undulator, *i.e.* modulator, and then the energy-modulated electron beams enter into a dispersive section where the energy modulation is converted into spatial modulation. Finally, the coherent emission at high harmonic of the seed laser generates in the second undulator, *i.e.* radiator.

A typical harmonic generation FEL scheme demonstrated experimentally is high gain harmonic generation (HGHG)<sup>[2]</sup> in the visible<sup>[6]</sup> and ultraviolet region<sup>[7]</sup>. Generally, the standard HGHG-FEL is limited by a low frequency multiplication factor to avoid a large modulation of beam energy. Thus, some novel harmonic generation FEL schemes are recently proposed so that the harmonic number can be up to several tens<sup>[8–12]</sup>.

FEL radiation is highly relevant with longitudinal distribution of the electron beam, especially in the frame of resonant wavelength. In the conventional model for harmonic generation FEL, the radiation evolutions in the modulator and radiator are determined by an averaged the electron behaviors over one seed laser wavelength.

When the frequency multiplication factor is low, such an approach is valid, and the model is simple and easy to solve. However, the longitudinal distribution of electron beam is not uniform over the distance of one seed laser wavelength after the density modulation. In the radiator, microstructures down to attosecond scale are produced, and this should be taken into account in the radiation evolution of radiator, especially in the case of high frequency multiplication factor.

In this paper, we developed a modified model for harmonic generation FEL, based on the undulator period-averaged approach and the micro-structures in one seed laser wavelength. The modified model is briefly described by employing a group parameter of Shanghai soft X-ray FEL (SXFEL)<sup>[13]</sup>, and is utilized

Supported by Shanghai Natural Science Foundation (Grant No. 09JC1416900).

\* Corresponding author. E-mail address: denghaixiao@sinap.ac.cn

Received date: 2009-09-08

to study the ultra-high order harmonic generation, the mode-locked FEL<sup>[8]</sup> and echo-enabled harmonic generation (EEHG) scheme<sup>[11,12]</sup>. The results show that the modified model is robust for handling FEL schemes with ultra-high order harmonic generation and ultra-short pulse.

## 2 Modified model for harmonic generation FEL

Generally, the electron bunch length is much larger than the seed laser wavelength, and the beam current variation in one seed laser wavelength can be neglected. Therefore, the longitudinal distribution of the initial beam can be written as

$$f(\gamma, \theta) = \frac{1}{\sqrt{2\pi}\sigma_\gamma} e^{-\frac{(\gamma-\gamma_0)^2}{2\sigma_\gamma^2}} \quad (1)$$

where,  $\sigma_\gamma$  is the RMS energy spread of the electron beam, and  $\gamma_0$  is the mean beam energy. After passing through various combinations of the modulator and the dispersive section, the longitudinal distribution of the electron beam can be written as

$$\begin{aligned} g(\gamma, \theta) &= G[f(\gamma, \theta)] \\ F(\theta) &= \int_{-\infty}^{\infty} g(\gamma, \theta) d\gamma \end{aligned} \quad (2)$$

where, the  $G$  function represents all effects to the longitudinal phase space before entering the radiator. For simplicity, here we just consider the electrons over the distance of one seed laser wavelength  $\lambda_s$ .

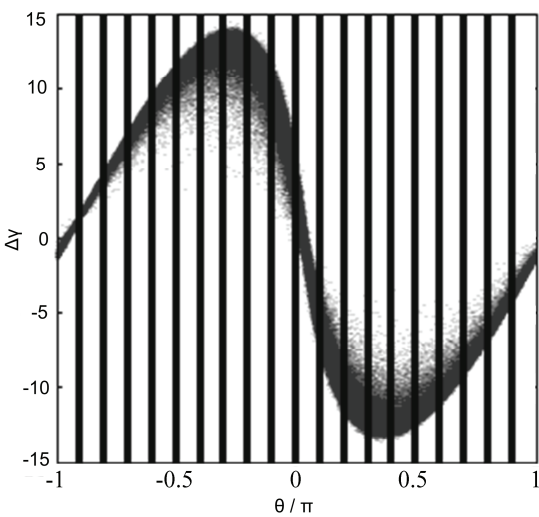


**Fig. 1** The longitudinal phase space of electron beam before entering the radiator in standard HGHG.

A resonance of radiator at the  $n$ -th harmonic of the seed is assumed in the following discussion. With the  $G$  function, the longitudinal density of the electron beam is no more uniform in  $[0, \lambda_s]$ , and the electrons in  $[0, \lambda_s]$  occupy  $n$  resonant wavelength of the radiator. As shown in Fig.1, the electrons are uniformly divided into  $n$  slices over the distance of  $\lambda_s$ , and the local current factor  $I_n(k)$  and local bunching factor  $B_n(k)$  are defined as,

$$I_n(k) = \frac{\int_{2k\pi/n-2\pi/n}^{2k\pi/n} F(\theta) d\theta}{2\pi/n} \quad (3)$$

$$B_n(k) = \frac{\int_{2k\pi/n-2\pi/n}^{2k\pi/n} F(\theta) e^{-in\theta} d\theta}{\int_{2k\pi/n-2\pi/n}^{2k\pi/n} F(\theta) d\theta} \quad (4)$$

where,  $k = 1, 2 \dots n$ .

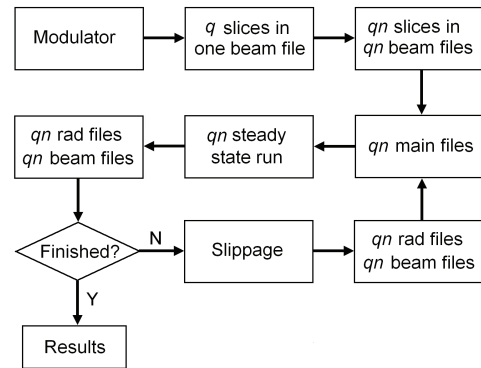


**Fig. 2** Process flow chart of the modified model for harmonic generation FEL scheme.

After passing one period of radiator, the radiation slips over the electron bunch by the distance of  $\lambda_s/n$ , and the electrons in each slice are independent with other slices. The radiation field  $E_n(k)$  in each slice is determined by  $I_n(k)$  and  $B_n(k)$ , thus one cannot average the electrons over one seed laser wavelength. After passing through  $n$  periods of radiator, electrons in one seed wavelength are correlated by the radiation slippages. However, all the longitudinal distribution of the electron beam varies through the radiator due to effects of the radiation and dispersion in the radiator. Thus, to appropriately describe a harmonic generation FEL in the radiator, the particle dynamics should be averaged over one radiator resonant wavelength instead of one seed wavelength.

Therefore, a modified numerical model for harmonic generation FEL scheme is developed. The

beam dynamics in the modulator and dispersive section are calculated by standard GENESIS<sup>[14]</sup>, as shown in Fig. 2. The steady-state run of GENESIS is used as a field solver for each beam slice in the radiator, and all the slippages are artificially processed in external of GENESIS after each period of radiator.

### 3 Examples and discussions

SXFEL<sup>[13]</sup> is a two-stage HGHG scheme, which is designed to generate 9 nm FEL from 270 nm seed laser. The main parameters of SXFEL are listed in Table 1. Three harmonic generation FEL examples are discussed by using the modified model and the SXFEL parameters.

**Table 1** The main parameters of SXFEL.

Parameters	Values
Electron beam energy E /GeV	0.84
Peak current I <sub>P</sub> /A	600
Normalized emittance ε /mm-mrad	2
Local energy spread σ <sub>y</sub> /γ	2×10 <sup>-4</sup>
Seed laser wavelength λ <sub>S</sub> /nm	270
Modulator period length λ <sub>UM</sub> /mm	58
Modulator undulator parameter K <sub>M</sub>	6.83
Modulator undulator periods	16
Radiator resonant wavelength λ <sub>R</sub> /nm	9
Radiator period length λ <sub>UR</sub> /mm	25
Radiator undulator parameter K <sub>R</sub>	1.41

#### 3.1 Ultra-high order harmonic generation

In the standard HGHG, after the dispersive section, the longitudinal distribution of the electron beam is

$$F(\theta) = 1 + 2 \sum_{m=1}^{\infty} e^{-(mD\sigma_y)^2/2} J_m[-mD\Delta\gamma] \cos m\theta \quad (5)$$

where, Δγ is the maximum energy modulation at the end of modulator, D is the dispersive strength contributed from the modulator and dispersive section. From Eq.(5), one may obtain

$$I_n(k) = 1 + \frac{2n}{\pi} \sum_{m=1}^{\infty} p_m b_m \quad (6)$$

$$B_n(k) = \frac{\sum_{m=1}^{\infty} q_m b_m}{\frac{\pi}{n} + 2 \sum_{m=1}^{\infty} p_m b_m} \quad (7)$$

where,

$$p_m = \frac{\cos \frac{2mk\pi}{n} \sin \frac{m\pi}{n}}{m}$$

$$q_m = e^{-2ik\pi} \left( \frac{e^{i2km\pi/n} \sin \frac{m-n}{n}\pi}{m-n} + \frac{e^{-i2km\pi/n} \sin \frac{m+n}{n}\pi}{m+n} \right)$$

$$b_m = e^{-(mD\sigma_y)^2/2} J_m[-mD\Delta\gamma]$$

In the case of harmonic generation scheme with low n, when the radiation slips forward the electron beam over λ<sub>s</sub> in radiator, the longitudinal distribution of the electron beam varies a little. Thus the local bunching factor can be averaged over the distance of λ<sub>s</sub>, and then Eq.(7) reduces to the universal form reported in Ref. [2,15].

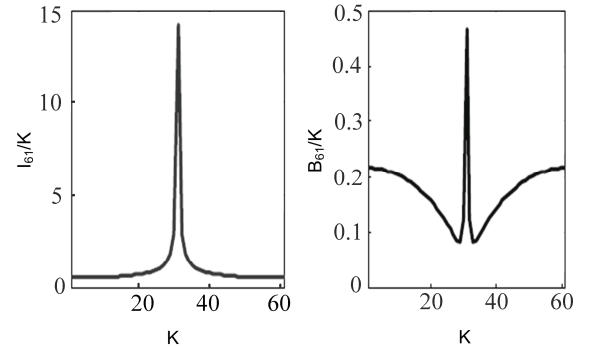


**Fig. 3** Estimated local current factor and local bunching factor of the 61<sup>th</sup> harmonic at the modulator exit.

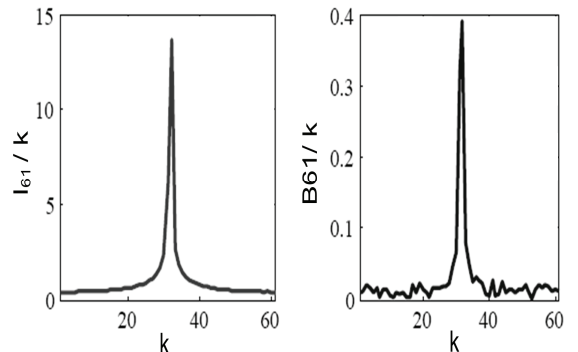


**Fig. 4** Simulated local current factor and local bunching factor of the 61<sup>th</sup> harmonic at the modulator exit.

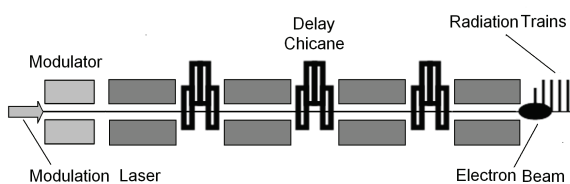
In the case of ultra-high harmonic, the Bessel function  $J_m(mx)$  has the maximum at  $x \approx 1$ . With a group of the optimized parameters, Fig. 3 shows the analytical results of SXFEL example with  $n = 61$ . When a strong energy modulation of  $\Delta\gamma = 16.3$  is

induced, at the exit of the dispersive section, most electrons are modulated to the position around  $k = 31$ , where the local beam current enhances 14 times more than the uniform current of the initial 600 A, and the local bunching factor is still 0.46.

To validate the analytical estimation, three-dimensional simulations were carried out and the results are shown in Fig. 4. With an energy modulation of  $\Delta\gamma = 21.2$ , the local current factor is about 13.5 and the local bunching factor is up to 0.39 at the position around  $k = 31$ . This consistency with the estimation indicates that the relativistic electron beam is modulated on attosecond scale so that it can produce ultra-high order harmonic generation of the seed laser within a very short radiator.

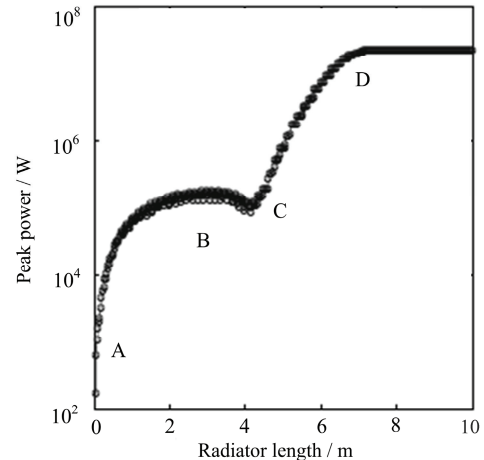
### 3.2 The mode-locked FEL

The mode-locked FEL<sup>[8]</sup> was proposed to generate attosecond radiation trains from a FEL amplifier. In the mode-locked FEL, a comb of longitudinal modes is synthesized by the optics-free technique applying a series of temporal shifts between the co-propagating radiation and electron bunch in a FEL amplifier. The longitudinal modes are phase-locked by inducing energy modulation from a seed. Fig. 5 shows a layout of the mode-locked FEL. More details can be found in Ref [8,16].



**Fig. 5** Schematic of the mode-locked FEL.

In SXFEL, the final radiation is the 30<sup>th</sup> harmonic of the 270 nm seed laser. If six periods is chosen in each segment of radiator and that a chicane is introduced to give an electron bunch delay of  $23 \lambda_R$ , the total slippage is  $29 \lambda_R \approx \lambda_S$  due to the undulator and chicane. Under such circumstances, SXFEL operates as a mode-locked FEL. An energy modulation with amplitude about 5 MeV is induced by seeding the modulator with a 5 GW and 270 nm laser. The modified model for harmonic generation FEL is used to study the evolution of 9 nm radiation in the mode-locked status of SXFEL.



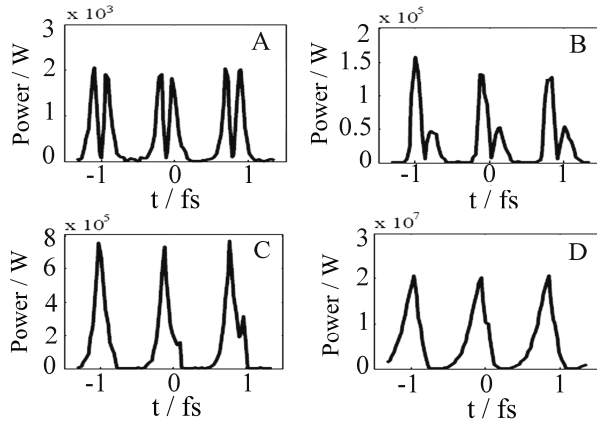
**Fig. 6** Peak power growth in the mode-locked SXFEL.

Fig. 6 illustrates the peak power growth in the radiator of the mode-locked SXFEL, from which it is seen that the peak power goes through a slow growth from A to B, a dramatic growth from C, and a final saturation at D. In order to understand the growth curve, the radiation pulses at different radiator position are given in Fig. 7. According to the temporal structures, it is known that the mode-locking competes with self-amplified spontaneous emission (SASE) from A to B, dominates at C and dramatically improves the temporal pulse structure. At the end of the radiator, 9 nm radiation trains with pulse width of 240 fs and peak power of 20 MW level are modeled, and evenly spaced by 0.9 fs (equal to 270 nm).

For mode-locked FEL, the modified model is capable for handling the details temporally shorter than one seed laser cycle, and it is easy to describe the pulse variations by using different chicane delays and tapered undulator sections. But this is beyond the scope of this paper.

### 3.3 Operating SXFEL with EEHG scheme

EEHG scheme has a remarkable bunching efficiency of frequency up-conversion and allows for generation a high harmonic beam density modulation with a relatively small energy modulation<sup>[11,12]</sup>. It has been shown that 9 nm coherent radiation with peak power about 400 MW can be directly generated from the 270 nm seed laser by operating SXFEL with EEHG scheme<sup>[17]</sup>. This was investigated by the modified model.



**Fig. 7** Radiation pulse structures of the mode-locked FEL.

The conventional model results a bunching parameter of 0.08 for the 30<sup>th</sup> harmonic in EEHG operation of SXFEL. In the modified model, the local current factor and the local bunching factor unevenly distributes in one seed laser wavelength at the entrance of the radiator, as seen in Fig. 8. The maximum of local current factor and the local bunching factor are about 1.3 and 0.2, respectively.

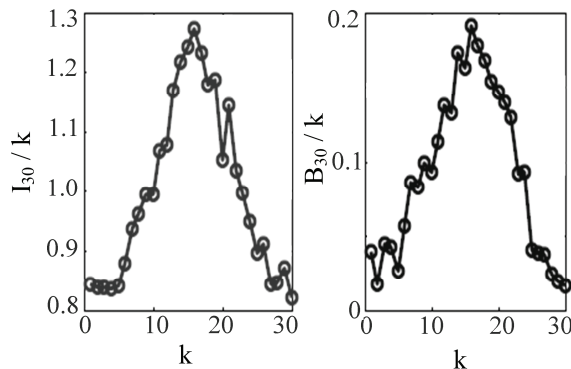


**Fig. 8** The local current factor and local bunching factor in one seed wavelength at the entrance of a 9 nm radiator, by running the SXFEL with EEHG scheme, obtained from the modified three dimensional simulations.

The peak power growth of the 9 nm radiation in the radiator is shown in Fig. 9. In the modified model, the peak power oscillates several times at the beginning of the radiator. This is contributed by the local bunching factors with opposite angles in two half-cycle of one seed wavelength. However, the saturation power is consistent in two different models.

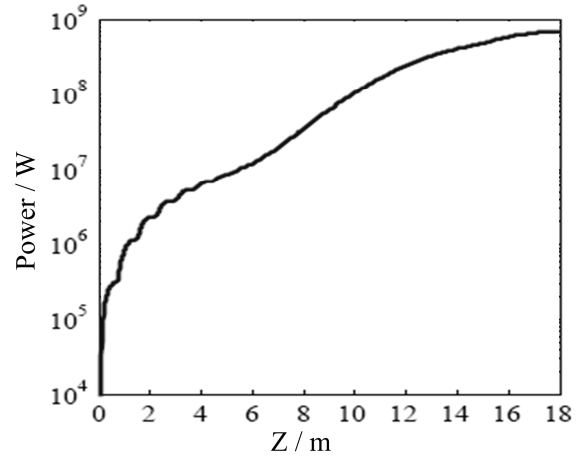


**Fig. 9** The growth of 9 nm peak power in the radiator.

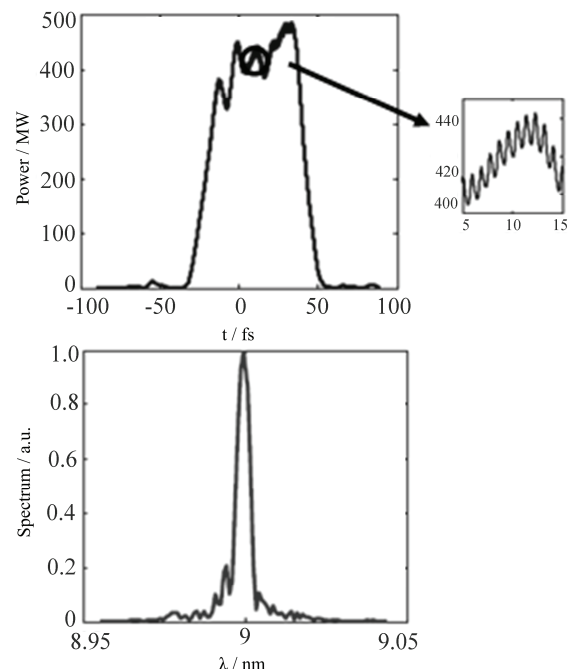


**Fig. 10** Temporal and spectral domain of final 9 nm radiation.

Fig. 10 illustrates the final 9 nm radiation pulse and spectra. The results are very similar to those of the conventional model. The enlarged section shows many small ripples with a period of 270 nm, a phenomenon that cannot be observed with a conventional model. If the 9 nm radiation pulse is introduced to other harmonic generation stage for further frequency multiplication, the ripples will be the input amplitude noise. This means that the modified model is more competent for noise propagation issue in harmonic generation FEL.

## 4 Conclusions

Based on the averaging of one seed laser wavelength, the conventional model for harmonic generation FEL smears and neglects the microstructures generated by density modulation in one seed laser wavelength. When one considers that the recently proposed FEL schemes involves with the ultra-high harmonic generation and ultra-short pulse, these microstructures are important and should be taken into account. Based on the averaged wavelength of the interested harmonic radiations, an upgraded and more realistic model for harmonic generation FEL is proposed, and three harmonic generation FEL examples are investigated and discussed by using SXFEL parameters. The modified model shows a robust capability to characterize FEL schemes with ultra-high harmonic generation and ultra-short pulse, and presents some new results which are helpful for understanding of radiation pulse evolution, bunching efficiency and noise propagation issues in FEL.

## References

- 1 Bonifacio R, Salvo L De, Pierini P, *et al.* Nucl Instrum Meth Phys Res A, 1990, **296**: 787–790.
- 2 Yu L H, Phys Rev A, 1991, **44**: 5178–5193.
- 3 Wu J H, Yu L H, Nucl Instrum Meth Phys Res A, 2001, **475**: 104–111.
- 4 Goloviznin V V, Van-Amersfoort P W, Phys Rev E, 1997, **55**: 6002–6010.
- 5 Deng H X, Dai Z M, Chin Phys C, 2008, **32**: 593–598.
- 6 Yu L H, Babzien M, Ben-Zvi I, *et al.* Science, 2000, **289**: 932–934.
- 7 Yu L H, DiMauro L, Doyuran A, *et al.* Phys Rev Lett, 2003, **91**: 074801.
- 8 Thompson N R, McNeil B W J, Phys Rev Lett, 2008, **100**: 203901.
- 9 Allaria E, Ninno G D, Phys Rev Lett, 2007, **99**: 014801.
- 10 Jia Q K, Appl Phys Lett, 2008, **93**: 141102.
- 11 Stupakov G, Phys Rev Lett, 2009, **102**: 074801.
- 12 Xiang D, Stupakov G, Phys Rev ST Accel Beams, 2009, **12**: 030702.
- 13 Kong X C, Wang J Q, Wang S H, *et al.*, Shanghai Soft X-ray FEL Test Facility Conceptual Design Report, 2008, Shanghai, Chapter 2: 1–20.
- 14 Reiche S, Nucl Instrum Meth Phys Res A, 1999, **429**: 243–248.
- 15 Jia Q K, Phys Rev ST Accel Beams, 2005, **8**: 060701.
- 16 McNeil B W J, Thompson N R, Dunning D J, *et al.* Proceeding of FEL08, Geyongju, Korea, 2008: 177–180.
- 17 Xiang D, Stupakov G, SLAC-PUB-13475, 2008.